Available online at www.sciencedirect.com
SCIENCE DIRECT®
Journal of Chromatography A, 997 (2003) 207–218
JOURNAL OF CHROMATOGRAPHY A
www.elsevier.com/locate/chroma

Mixed-mode electrokinetic chromatography of aromatic bases with two pseudo-stationary phases and pH control

Philip Zakaria, Miroslav Macka, Paul R. Haddad*
Department of Chemistry, University of Tasmania, GPO Box 252-75, Hobart, Tasmania 7001, Australia

Abstract

The electrokinetic chromatographic (EKC) separation of a series of aromatic bases was achieved utilising an electrolyte system comprising an anionic soluble polymer (polyvinylsulfonic acid, PVS) and a neutral β-cyclodextrin (β-CD) as pseudo-stationary phases. The separation mechanism was based on a combination of electrophoresis, ion-exchange interactions with PVS, and hydrophobic interactions with β-CD. The extent of each chromatographic interaction was independently variable, allowing for control of the separation selectivity of the system. The ion-exchange and the hydrophobic interactions could be varied by changing the PVS and the β-CD concentrations, respectively. Additionally, mobilities of the bases could be controlled by varying pH, due to their large range of pK_a values. The separation system was very robust with reproducibility of migration times being <2% RSD. The two-dimensional parameter space defined by the two variables, [β-CD] and %PVS, was modelled using a physical model derived from first principles. This model gave very good correlation between predicted and observed mobilities (r^2=0.999) for the 13 aromatic bases and parameters derived from the model agreed with the expected ion-exchange and hydrophobic character of each analyte. The complexity of the mathematical model was increased to include pH and this three-dimensional system was modelled successfully using an artificial neural network (ANN). Optimisation of both the two-dimensional and three-dimensional systems was achieved using the normalised resolution product and minimum resolution criteria. An example of using the ANN to predict conditions needed to obtain a separation with a desired migration order between two of the analytes is also shown.

Keywords: Mixed-mode separations; Electrokinetic chromatography; Neural networks, artificial; Pseudo-stationary phases; Pyridines; Anilines; Amines; Picoline; Quinoline

1. Introduction

Capillary electrophoresis (CE) is a powerful technique for the separation of charged species [1], with separation occurring due to differences in electrophoretic mobilities of the analytes being investigated. CE has several advantages over more traditional chromatographic methods such as ion chromatography (IC) and high-performance liquid chromatography (HPLC), including high efficiency, reduced analysis time and smaller sample volumes. However, a general limitation of CE is the lack of a convenient method to change the separation selectivity of the system. Since separation is achieved by differences in effective electrophoretic mobilities between the analytes, the only way to alter the observed selectivity is to change these mobilities. This can be achieved by altering background electrolyte (BGE) conditions such as pH, ionic strength, organic modifier content

*Corresponding author. Tel.: +61-3-6226-2179; fax: +61-3-6226-2858.
E-mail address: paul.haddad@utas.edu.au (P.R. Haddad).

0021-9673/03/$ – see front matter
doi:10.1016/S0021-9673(03)00064-5

[2], etc. Normally, these changes only bring about relatively small changes in selectivity.

A complimentary technique that offers additional options for selectivity control is electrokinetic chromatography (EKC). In EKC a pseudo-stationary phase (pseudo-SP) is added to the CE system to interact with the analytes, often providing a selectivity which differs from that of CE. EKC potentially offers control in selectivity similar to capillary electrochromatography (CEC), where a solid SP is packed or chemically bound within a capillary, but is far simpler to operate since no packing procedures are required and there is no necessity for retaining frits.

Pseudo-SPs for EKC can be formed by adding a suitable component to the BGE. A wide variety of pseudo-SPs is available and the only prerequisite of the SP is that it should be soluble in the BGE. The majority of published work on pseudo-SPs has focused on the use of micelles (anionic, cationic, zwitterionic and neutral) but several other phases have also been investigated [2–4]. The choice of pseudo-SP depends on the analytes of interest and the desired mechanism of interaction with the analytes (ion-exchange, chelation, hydrophobicity, etc.).

In a simple EKC system consisting of a single pseudo-SP interacting with the analytes via a single mechanism, the selectivity can only be modified using that mechanism of interaction, i.e. in a one-dimensional manner. The separation selectivity (and hence the observed migration order) can be varied between that of a pure CE system and that of the corresponding chromatographic system. If a further interaction mechanism is introduced, either with the same pseudo-SP or by addition of an additional pseudo-SP, the selectivity of the system can potentially now be varied in a two-dimensional manner which should permit a higher degree of control of selectivity. The preferred implementation of such a system is for each interaction to be independently variable since this would allow the extent of each interaction to be varied without influencing any other interactions with analytes which occur in the system. This requires that two or more pseudo-SPs, each exhibiting a different interaction with the analytes, be added to the BGE. Work within this laboratory has already demonstrated such a system for the separation of inorganic and small organic anions [5] where a soluble cationic polymer poly-(diallydimethylammonium chloride) (PDDAC) and β-cyclodextrin (β-CD) were used as pseudo-SPs. Separation of the analyte anions was based on differences in electrophoretic mobility, ion-exchange affinities for the cationic polymer and hydrophobic partitioning into the cyclodextrin cavity. The extent of the ion-exchange interaction could be varied by either changing the PDDAC concentration or the concentration of a competing anion in the BGE, whilst the extent of the analyte–CD interaction could be varied by changing the concentration of the β-CD in the BGE.

Separation of various substituted anilines and pyridines has been reported using small ionic additives such as ethane- and propanesulfonic acids [6,7], polyethylene glycol [8], various anionic surfactants [9] and mixed systems comprising surfactants with tetraalkylammonium salts [10] and surfactants with cyclodextrins [11,12]. However, these systems offer only limited control of selectivity because only one type of chromatographic interaction is generally used to gain separation. The aim of the present work was to extend the current ion-exchange/hydrophobic system to the separation of cations by establishing a mixed-mode separation for a series of aromatic anilines and pyridines using the soluble anionic polymer polyvinylsulfonate (PVS) and the neutral β-CD as pseudo-SPs. A mathematical model as well as an artificial neural network (ANN) were also investigated as tools for optimisation of the resultant system.

2. Experimental

2.1. Instrumentation

The CE instrument used was a Hewlett-Packard ^{3D}CE (Waldbronn, Germany). Separations were carried out using Polymicro (Phoenix, AZ, USA) fused-silica capillaries (50 cm (41.5 cm to detector)×50 μm I.D.) Injection was performed by applying 50-mbar pressure for 5 s to the injection side of the capillary. Separations were performed in the co-EOF mode, i.e. with migration of both the analytes and the EOF being towards the negative electrode, using detection by direct spectrophotometry at between

200 and 211 nm. All separations were performed at +15 kV.

2.2. Capillary coating procedures

A capillary showing pH independent electroosmotic flow (EOF) based on work by Katayama et al. [13] was used for this study; the procedure for its preparation has been reported previously [14]. Briefly, this involved first coating a fused-silica capillary with the cationic polymer PDDAC followed by coating with the anionic polymer dextran sulfate. This resulted in a positive EOF (i.e. towards the negative electrode) which was independent of pH over the range 2.5–7.5.

2.3. Reagents

Analytical-grade citric acid and sodium citrate were obtained from Sigma–Aldrich (Milwaukee, WI, USA) and used without further purification. PVS was obtained as a 25% (w/v) solution and PDDAC, with a molecular mass of 400 000–500 000, as a 20% (w/v) solution. β-CD was obtained from Sigma–Aldrich. All chemicals were used without further purification.

Cation standards of 10 m*M* concentration (pyridine, picoline, 4-ethylpyridine, 4-*tert*.-butylpyridine, quinoline, *p*-aminopyridine, *m*-aminopyridine, *o*-aminopyridine, aniline, 4-ethylaniline, 4-pentylaniline, benzylamine and 4-methylbenzylamine) were prepared in water. HCl was added to dissolve some of the less soluble bases. BGEs were prepared by mixing 100 m*M* stock solutions of citric acid and sodium citrate in varying ratios to produce 20 m*M* citrate electrolytes of varying pH. β-CD was dissolved in each electrolyte to give the desired concentration. All electrolytes were degassed using an ultrasonic bath for 2 min prior to use. EOF values were determined by injecting acetone.

2.4. Artificial neural networks

Calculations involving ANN were performed using the Trajan Neural Network Simulator, Release 3.0 (Trajan Software, Durham, UK).

3. Results and discussion

3.1. Choice of analytes

The two main analyte interactions in the separation system were expected to be ion-exchange interactions with the PVS and hydrophobic partitioning with the β-CD. As such, analytes which exhibit differences both in cation-exchange selectivity and/or hydrophobicity should be applicable to the current system. A series of test analytes comprising anilines, pyridines and benzylamines was chosen and these are listed in Table 1, together with their pK_a values. The different molecular groups (anilines, pyridines and amines) should exhibit different ion-exchange affinities for the PVS, while the different alkyl substituents should lead to differing affinities for the β-CD. The wide range of pK_a values also permits pH to be used as a further variable to control the selectivity.

3.2. Selectivity

Separations of anions performed using PDDAC as a pseudo-SP showed that hydrophobic interactions between this polymer and small organic anions were very weak [5]. It therefore can be reasonably assumed that PVS would also show only very weak hydrophobic interactions and should exhibit predominantly ion-exchange interactions with small

Table 1
Test analytes and associated pK_a values

Analyte	pK_a
Pyridine	5.17
Picoline	6.00
4-Ethylpyridine	5.87
4-*tert*.-Butylpyridine	5.99
Quinoline	4.80
p-Aminopyridine	9.11
m-Aminopyridine	6.03
o-Aminopyridine	6.71
Aniline	4.60
4-Ethylaniline	5.00
4-Pentylaniline	5.10[a]
Benzylamine	9.35
4-Methylbenzylamine	9.52[a]

[a] Calculated using ACD/pK_a v4.56, Advanced Chemistry Development, Toronto, Canada.

organic cations. This can be seen in Fig. 1 which shows the effect of adding 2% (w/v) PVS to the BGE. It can be seen that the addition of PVS decreased the mobility of all the analytes, with the magnitude of this interaction differing between analytes and therefore leading to changes in selectivity. It is also evident that addition of PVS to the BGE affected the anilines and benzylamines more than the pyridines, indicating that pyridines had the weakest interactions with PVS.

If the interaction between PVS and the bases was predominantly ion-exchange in nature, increasing the concentration of the competing ion in the BGE should decrease these interactions. A similar effect should be observed if the competing ion was replaced by a stronger competing ion, for example by replacing a monovalent competing ion with a divalent ion. Fig. 2 shows the effect of increasing the concentration of the competing ion and also changing the competing ion from Na^+ to Mg^{2+}. In accordance with the predicted ion-exchange mechanism, the mobilities of all analytes increased with increasing competing ion concentration and Mg^{2+} produced more pronounced changes in analyte mobility than Na^+ due to the stronger ion-exchange interactions of the divalent Mg^{2+}.

It can be expected that the addition of β-CD to the BGE should have a greater effect on the more hydrophobic analytes. This effect has been demonstrated in a previous paper on modelling the separation of aromatic bases using β-CD [14].

For the proposed system to be practically useful,

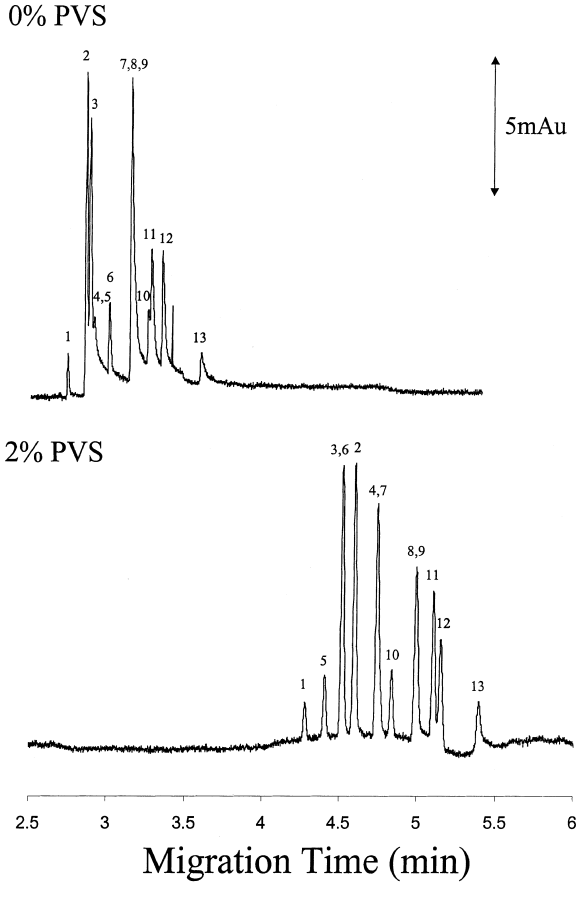

Fig. 1. Effect of %PVS on the separation of the 13 aromatic bases. Peaks are: 1 = pyridine, 2 = *m*-aminopyridine, 3 = *p*-aminopyridine, 4 = *o*-aminopyridine, 5 = picoline, 6 = ethylpyridine, 7 = quinoline, 8 = aniline, 9 = benzylamine, 10 = *tert.*-butylpyridine, 11 = methylbenzylamine, 12 = ethylaniline and 13 = pentylaniline. Conditions: 20 m*M* citrate BGE, pH 3.50, detection at 208 nm.

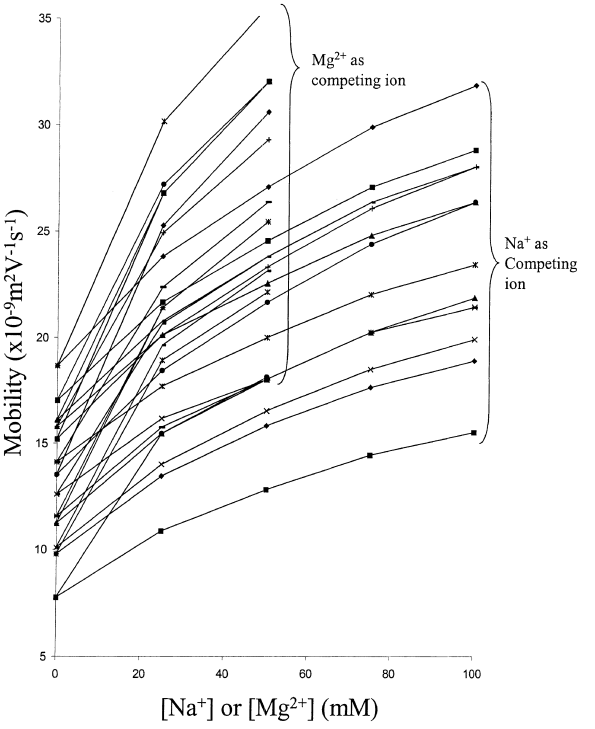

Fig. 2. Effect of competing-ion type and concentration on the separation of aromatic bases. Conditions: 20 m*M* citrate BGE, pH 3.50.

both the ion-exchange and hydrophobic interactions should be independent so that varying the extent of one interaction should have little effect on the other. In the previous work with anions [5], an equivalent separation system comprising PDDAC and β-CD did exhibit independent ion-exchange and hydrophobic interactions. It can be reasonably assumed that the current system should also exhibit independent interactions.

The use of aromatic bases having a large range of pK_a values (Table 1) allows pH to be employed as an additional parameter to control selectivity. The effect of pH on the hydrophobic interaction between the analytes and β-CD has been described in a previous paper [14] where it was shown that the interaction between the neutral form of the analyte and the β-CD was stronger than the interaction between the charged form of the analyte and the β-CD. Thus, varying pH not only modifies the extent of ionisation of the analytes, but also affects interactions of the analytes with β-CD. In a similar way it can be expected that by altering the extent of ionisation of the bases, the ion-exchange interactions with the PVS will also vary since only the protonated base will undergo ion-exchange interactions. The complete separation system is shown schematically in Fig. 3a, with the three experimentally variable parameters being the concentrations of PVS and β-CD and the pH.

Under a given set of experimental conditions, the system exhibited good reproducibility with migration times for the analytes varying by less than 2% RSD over 15 consecutive 10-min runs. The capillary coating used was also very stable with the migration time of the EOF varying by less than 2.4% RSD over the same set of runs.

3.3. Simplified modelling of the system

From Fig. 3a, it can be seen that the complete separation system was relatively complex and involved four simultaneous equilibria. Modelling this system by deriving a mathematical model from first principles would be relatively complex, and for this reason a simplification of the system was considered first. This involved removing pH as a variable, leading to the separation system shown in Fig. 3b.

a.

$$\begin{array}{ccc} & BH^+_{cd} & \\ & K_{cd+} \Updownarrow & \\ BH^+_{bge} + E^+_{pvs} & \overset{K_{pvs}}{\rightleftharpoons} & BH^+_{pvs} + E^+_{bge} \\ K_a \Updownarrow & & \\ B_{bge} & \overset{K_{cd}}{\rightleftharpoons} & B_{cd} \\ + & & \\ H^+_{bge} & & \end{array}$$

b.

$$\begin{array}{ccc} & BH^+_{cd} & \\ & K_{cd+} \Updownarrow & \\ BH^+_{bge} + E^+_{pvs} & \overset{K_{pvs}}{\rightleftharpoons} & BH^+_{pvs} + E^+_{bge} \end{array}$$

Fig. 3. Schematic showing the likely equilibrium processes present in the current system. (a) Three-dimensional system with the variables being [PVS], [β-CD] and pH. (b) Simplified two-dimensional system excluding pH as a variable. In this system the pH is maintained sufficiently low so that all bases are fully protonated. K_{pvs} is the ion-exchange selectivity coefficient between the analytes and the PVS. K_{cd} and K_{cd+} are the equilibrium constants between the β-CD and the neutral and protonated base, respectively. B and BH^+ represent the neutral and protonated base, respectively. E^+ represents the competing ion (Na^+ for the work presented here). The subscripts bge, pvs and cd refer to the appropriate species in the background electrolyte, PVS or cyclodextrin phases, respectively.

The pH in this simplified system was maintained at pH 3.50 to ensure that all the bases were protonated fully.

The equilibria shown in Fig. 3b are characterised by the equilibrium constants K_{cd+} and K_{pvs} with the former being a hydrophobic interaction constant between the protonated analyte and the β-CD and the latter being the ion-exchange selectivity coefficient describing the ion-exchange competition for the PVS pseudo-SP between the protonated analyte and the eluent competing cation (E^+). These equilibria are defined as:

$$K_{cd+} = \frac{[BH^+]_{cd}}{[BH^+]_{bge}} \quad (1)$$

$$K_{pvs} = \frac{[BH^+]_{pvs}[E^+]_{bge}}{[BH^+]_{bge}[E^+]_{pvs}} \quad (2)$$

where $[BH^+]_{bge}$, $[BH^+]_{pvs}$ and $[BH^+]_{cd}$ refer to the concentrations of the protonated analyte in the BGE, PVS and cyclodextrin phases, respectively. $[E^+]_{bge}$ and $[E^+]_{pvs}$ refer to the concentration of the competing ion (in this work Na^+) in the BGE and PVS phases, respectively.

Retention factors for both the cyclodextrin and PVS can be determined. In the case of PVS this can be derived from ion-chromatography theory [5],

$$k'_{poly} = \frac{w_{poly}}{V_{bge}} \cdot (K_{poly})^{1/y} (Q/y)^{x/y} [E^+]^{-x/y} \quad (3)$$

where w_{poly} is the mass of the PVS pseudo-SP, V_{bge} is the volume of the electrolyte, Q is the ion-exchange capacity of the ion-exchange pseudo-SP, $[E^+]$ is the concentration of the competing ion, while x and y are the charges on the analyte and eluent ion, respectively (both 1 in the current work).

An equivalent expression for k'_{cd} can be derived from first principles [5]:

$$k'_{cd} = \frac{V_{cd}}{V_{bge}} \cdot K_{cd+} \quad (4)$$

where V_{bge} and V_{cd} are the volumes of the BGE and cyclodextrin phases, respectively.

For two independent pseudo-SPs the total retention factor, k'_t of the system can be represented as a combination of the individual retention factors,

$$k'_t = k'_{cd} + k'_{pvs} \quad (5)$$

substituting for k'_{cd} and k'_{pvs} in Eq. (5) leads to a final expression for the retention factor of the system,

$$k'_t = \left(\frac{V_{cd}}{V_{bge}}\right) \cdot K_{cd+} + w_{\%} K_{pvs} Q [E^+]^{-1} \quad (6)$$

where $w_{\%}$ is now the mass percent of polymer in the BGE. The observed mobility of an analyte can be expressed in terms of this retention factor [15],

$$\mu_{obs} = \frac{1}{1+k'} \cdot \mu_{bge} + \frac{k'}{1+k'} \cdot \mu_{sp} \quad (7)$$

where μ_{obs} is the observed mobility of the analyte while μ_{bge} and μ_{sp} are the mobilities of the analytes in the electrolyte and pseudo-SP, respectively. Expanding the second term of Eq. (7) to accommodate the two independent pseudo-SPs gives:

$$\mu_{obs} = \frac{1}{1+k'_t} \cdot \mu_{bge} + \frac{k'_{cd}}{1+k'_{cd}} \cdot \mu_{cd} + \frac{k'_{pvs}}{1+k'_{pvs}} \cdot \mu_{pvs} \quad (8)$$

where μ_{cd} and μ_{pvs} are the mobilities of the analytes in the cyclodextrin and PVS phases, respectively. Expanding Eq. (8) by including previous equations gives a final equation for the separation.

Initial application of this equation to the separation of the 13 bases, however, showed that the $[E^+]^{-1}$ relationship, from Eq. (6), did not accurately represent the observed trends in μ_{obs}. This is in agreement with results found for the ion-exchange separation of cationic opiate compounds using a sulfated cyclodextrin as a pseudo-SP [16]. Replacing this with an $[Na^+]^{-x}$ term, Eq. (9), dramatically improved the results allowing the model to accurately predict the observed separations of the 13 bases. This outcome is most probably due to the fact that the displacement of Na^+ ions by the bases is not a 1:1 process, as assumed from ion chromatographic theory. This might be attributable to the fluid nature of the polymer which could cause some of the sulfonate ion-exchange sites to be inaccessible to the bases at various times. Since the exact displacement ratio will depend on a range of parameters and will be difficult to predict, its value was determined by non-linear regression, together with other unknown parameters in Eq. (9),

$$\mu_{obs} = \frac{1}{1+\left(\frac{V_{cd}}{V_{bge}}\right) \cdot K_{cd+} + w_{\%} K_{pvs} Q [Na^+]^{-x}} \cdot \mu_{bge} + \frac{\left(\frac{V_{cd}}{V_{bge}}\right) \cdot K_{cd+}}{1+\left(\frac{V_{cd}}{V_{bge}}\right) \cdot K_{cd+}} \cdot \mu_{cd} + \frac{w_{\%} K_{pvs} Q [Na^+]^{-x}}{1 + w_{\%} K_{pvs} Q [Na^+]^{-x}} \cdot \mu_{pvs} \quad (9)$$

In Eq. (9), $w_{\%}$ is defined by the %(w/v) of PVS in

the BGE. Q is also related to the %PVS and can be estimated by the number of repeat units in the polymer. V_{cd} can be estimated from the individual cavity volume of each β-CD molecule (0.346 nm^3) [17]. $[E^+]$ is defined by the concentration of sodium citrate added to the BGE while the remaining parameters, K_{cd+}, K_{pvs}, μ_{bge}, μ_{cd} and μ_{pvs} must be determined by non-linear regression. Non-linear regression was performed using the solver function in Microsoft Excel 97 for all analytes simultaneously, by a minimisation of least squares, similar to the process described previously [5].

3.4. Application of the simplified migration model

Eq. (9) contains six unknowns, K_{cd+}, K_{pvs}, μ_{bge}, μ_{cd}, μ_{pvs} and x. Normally at least seven experimental points would be required to estimate these constants, but it should be recognised that three of these constants (K_{cd+}, K_{pvs} and μ_{bge}) are specific to a particular analyte, while the remainder relate to the separation system and remain the same for all analytes. This permits the use of fewer experimental points when solving the equation and five experimental points comprising the four corner points and centre point of the two-dimensional experimental space defined by 0–1% (w/v) PVS and 0–10 m*M* β-CD were used. These points were termed the primary data set. A further eight points within the experimental space, termed the validation set, were used to evaluate the predictive power of the model.

Table 2 shows the constants obtained from the non-linear regression of Eq. (9) using the primary data set. The constants obtained in this way agreed with expected trends, especially the K_{cd+} values. Values within each group increased with increasing alkyl chain length for all classes of compounds (i.e. pyridines, anilines and benzylamines). The largest values of K_{cd+} were obtained for *tert*.-butylpyridine, ethylaniline and pentylaniline. It can also be seen that anilines exhibited slightly larger K_{cd+} values than the corresponding pyridines, indicating slightly stronger interactions with the β-CD. It should be noted that although the analyte–cyclodextrin interaction has been described as a hydrophobic interaction, it is possible that other interactions, e.g. host–guest complexation, hydrogen bond acceptor, etc., occur simultaneously, hence the K_{cd+} terms may cover more than simply hydrophobic interactions. Values obtained for K_{pvs} also agreed with the expected trends. The largest values were observed for the aminopyridines and benzylamines, while the lowest values were for the alkyl-substituted pyridines, in agreement with Fig. 1. It is also interesting to note that values of K_{pvs} decreased with increasing alkyl chain length, implying that the alkyl substituent exerted some hindering affect on the ion-exchange interaction with PVS. These results also showed that it was unlikely that the PVS exhibited any significant hydrophobic interaction with the analytes since this would result in an increase in K_{pvs} values with increasing alkyl chain length on the analyte.

Table 2
Constants determined using non-linear regression and the primary data set

Analyte	K_{pvs}	K_{cd+}	μ_{bge}[a]
Pyridine	4.69	1.32	40.6
Picoline	4.16	1.46	35.9
4-Ethylpyridine	4.05	1.84	33.4
4-*tert*.-Butylpyridine	4.00	66.91	27.7
Quinoline	3.81	3.42	30.2
o-Aminopyridine	5.47	1.47	35.9
m-Aminopyridine	5.12	1.31	37.4
p-Aminopyridine	4.65	1.39	36.7
Aniline	4.80	3.42	30.2
4-Ethylaniline	4.74	32.94	25.8
4-Pentylaniline	3.95	499.20	21.3
Benzylamine	4.95	3.42	30.2
4-Methylbenzylamine	4.78	9.7	27.3
μ^a_{pvs}	−22.7		
μ^a_{cd}	7.3		
x	2.1		

[a] $\cdot 10^{-9}$ m^2 V^{-1} s^{-1}.

System constants obtained were also within expected ranges. The mobility of the analyte–PVS complex would be expected to be negative since the overall charge on the PVS will remain negative even during interaction with the bases. This was reflected in the observed value of $-22.7 \cdot 10^{-9}$ m^2 V^{-1} s^{-1} for μ_{pvs}. It was also expected that the mobility of the analyte–CD complex would be greater than zero, but substantially lower than the mobility of the free

analytes. The observed value of $+7.3\cdot10^{-9}$ m^2 V^{-1} s^{-1} for μ_{cd} supported this hypothesis. The x value obtained was close to 2 implying a squared relationship between μ_{obs} and $[E^+]$. Interestingly this value was exactly the same as that obtained when modelling the ion-exchange separation of cationic opiate compounds using a sulfated cyclodextrin as a pseudo-SP [16].

Fig. 4 shows the correlation obtained between the observed and predicted mobilities for the entire data set, i.e. 169 points. It can be seen that a high degree of correlation was obtained with an r^2 value of 0.999.

3.5. Optimisation of separation conditions using the simplified model

Having an accurate model capable of predicting mobilities allows for the system to be optimised using an appropriate algorithm. This optimisation was performed using both the normalised resolution product criterion,

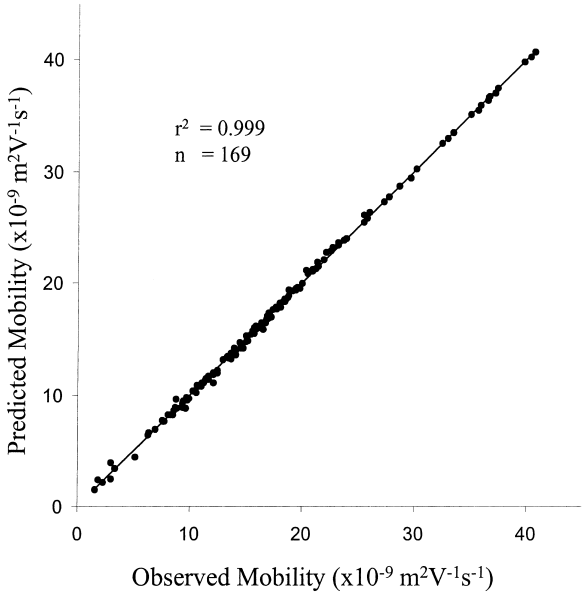

Fig. 4. Correlation between observed and predicted mobilities using Eq. (9) and constants shown in Table 2. Points used to derive constants also shown.

$$r_{min} = \prod_{i=1}^{n=1} \left(\frac{R_{s(i,i+1)}}{\frac{1}{n-1} \sum_{i=1}^{n-1} R_{s(i,i+1)}} \right) \quad (10)$$

and the minimum resolution criterion,

$$r_{min} = \min \left(\sum_{i=1}^{n-1} R_{s(i,i+1)} \right) \quad (11)$$

where $R_{s(i,i+1)}$ is the resolution between adjacent peaks and n is the number of peaks in the separation. r ranges from 0 to 1, with the best separation obtained for a value of 1. The normalised resolution product criterion is maximised when analyte peaks are spread evenly over the entire separation window, whereas the minimum resolution criterion simply considers the peak pair giving the worst resolution. To optimise the system resolution values were calculated over the selected experimental space. A separation was then run under the conditions predicted to yield the largest value of r. Observed migration times were then compared to those predicted by the model and a new optimum calculated and the separation run again. Again, predicted and observed migration times were compared and if the discrepancies exceeded 5%, the process was repeated until satisfactory agreement between predicted and experimental values was obtained.

Using this process optimal conditions were calculated to be 0 m*M* β-CD–1.0% PVS and 2.0 m*M* β-CD–0.95% PVS for the normalised resolution product and minimum resolution criteria, respectively. Separations performed under both these sets of conditions are shown in Fig. 5. It can be seen that both conditions led to at least partial separation of all analytes, with the normalised resolution product criterion yielding the better separation (Fig. 5a). The agreement between observed and predicted migration times for both optima was less than 1% for most analytes (23 of the 26 peaks) and less than 2.6% for the other three. It should also be noted that the separation between aniline and benzylamine will always be problematic using only %PVS and [β-CD] as variables since these analytes exhibit identical K_{cd+} and μ_{bge} values and very similar K_{pvs} values. It can be seen that both criteria utilise high levels of PVS trying to exploit this small difference. This problem is potentially avoidable if pH is used as an

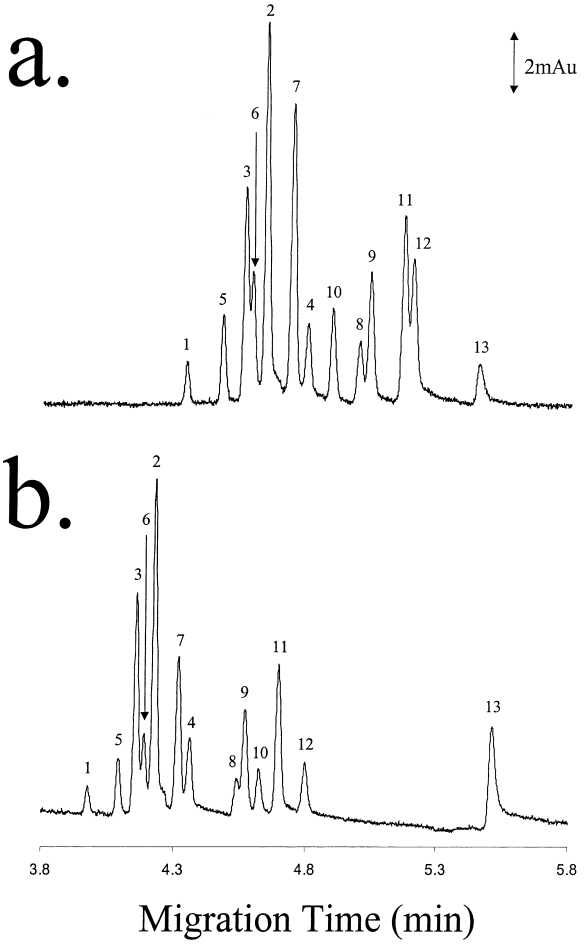

Fig. 5. Optimal separations calculated with Eq. (9) and using (a) the normalised resolution product criterion and (b) the minimum resolution criterion. Conditions: (a) 0 m*M* β-CD and 1.0% PVS; (b) 2.0 m*M* β-CD and 0.95% PVS. Peaks are: 1=pyridine, 2=*m*-aminopyridine, 3=*p*-aminopyridine, 4=*o*-aminopyridine, 5=picoline, 6=ethylpyridine, 7=quinoline, 8=aniline, 9=benzylamine, 10=*tert*.-butylpyridine, 11=methylbenzylamine, 12=ethylaniline and 13=pentylaniline. General conditions: 20 m*M* citrate, pH 3.50, detection at 200 nm.

experimental variable since these two analytes have very different pK_a values (4.60 and 9.35 for aniline and benzylamine, respectively).

3.6. Full modelling of the system

Inclusion of pH as a variable in the system has a complicating effect on the interactions of the analytes with both β-CD and PVS, as discussed earlier. However, in previous work we have successfully modelled the interactions of the analytes with β-CD under conditions of varying pH [14], using the model shown in Eq. (12):

$$\mu_{\text{obs}} = \frac{\alpha}{\sqrt{\text{pH}}} \cdot \left(\frac{1}{1+k'} \cdot b_{\text{bge}} + \frac{k'}{1+k'} \cdot \alpha b_{\text{cd}} \right) \quad (12)$$

where

$$k' = \left(\frac{V_{\text{cd}}}{V_{\text{bge}}} \right) \cdot \left(\frac{K_{\text{cd}} + 10^{(\text{p}K_{\text{a}} - \text{pH})} K_{\text{cd}+}}{1 + 10^{(\text{p}K_{\text{a}} - \text{pH})}} \right)$$

and

$$\alpha = \left(\frac{10^{(\text{p}K_{\text{a}} - \text{pH})}}{1 + 10^{(\text{p}K_{\text{a}} - \text{pH})}} \right)$$

In these equations K_{cd} and $K_{\text{cd}+}$ are the interaction constants between the β-CD and the neutral and protonated analytes, respectively. b_{bge} and b_{cd} are constants relating to the mobilities of the free protonated analytes and the complex formed between the protonated analyte and β-CD, respectively. V_{cd} and V_{bge} refer to the total volume of the cyclodextrin phase and BGE, respectively.

Assuming independent interactions between the analytes and the two pseudo-SPs, Eq. (12) can be extended to include the effect of PVS with the final model shown in Eq. (13):

$$\mu_{\text{obs}} = \frac{\alpha}{\sqrt{\text{pH}}} \cdot \left(\frac{1}{1 + k'_{\text{cd}} + k'_{\text{pvs}}} \cdot b_{\text{bge}} + \frac{k'_{\text{cd}}}{1 + k'_{\text{cd}}} \cdot \alpha b_{\text{cd}} + \frac{k'_{\text{pvs}}}{1 + k'_{\text{pvs}}} \cdot \alpha b_{\text{pvs}} \right) \quad (13)$$

where

$$k'_{\text{cd}} = \left(\frac{V_{\text{cd}}}{V_{\text{bge}}} \right) \cdot \left(\frac{K_{\text{cd}} + 10^{(\text{p}K_{\text{a}} - \text{pH})} K_{\text{cd}+}}{1 + 10^{(\text{p}K_{\text{a}} - \text{pH})}} \right)$$

and

$$k'_{\text{pvs}} = w_{\%} K_{\text{pvs}} Q [E^+]^{-1} \cdot \left(\frac{10^{(\text{p}K_{\text{a}} - \text{pH})}}{1 + 10^{(\text{p}K_{\text{a}} - \text{pH})}} \right)$$

All the parameters in Eq. (13) have been defined previously.

3.7. Application of the full migration model

Eq. (13) utilises the experimental parameters %PVS, [β-CD] and pH. As such, a three-dimensional experimental space defined by the variables 0–1% PVS, 0–10 m*M* β-CD and pH 3.5–7.2 was chosen. Initially, experimental conditions at the eight corner points and the centroid point were chosen as the primary data set, but this led to relatively poor predictability of observed migration times for a further 12 points contained within the experimental space with $r^2 = 0.937$ for the correlation between observed and predicted mobilities; this corresponded to differences in observed and predicted mobilities of up to $\pm 12 \cdot 10^{-9}$ m^2 V^{-1} s^{-1}. Correlation was improved ($r^2 = 0.986$) when a more complete set of 21 points was used as the primary data set (Fig. 6), but was inadequate to enable sufficiently accurate prediction of migration times for optimisation purposes (i.e. <5% error). The cause of this is the complexity of the three-dimensional model and the relatively large number of constants which need to be calculated. This limits the use of non-linear regression.

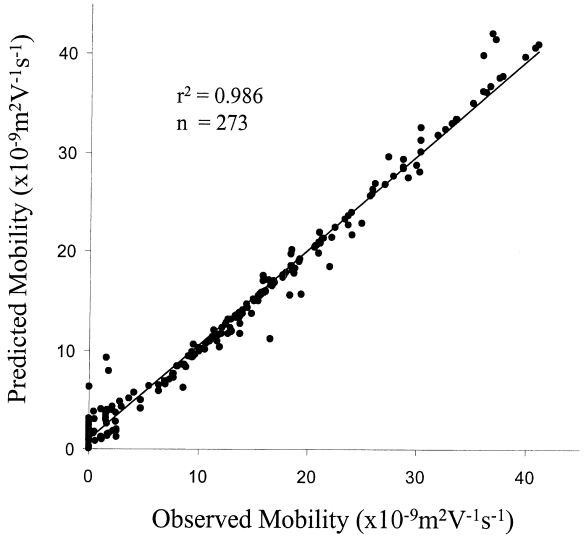

Fig. 6. Correlation between observed and predicted mobilities using Eq. (13) and 21 different conditions within the experimental space. All points shown were used to derive the constants for the model.

3.8. Artificial neural networks

Since the separation system could not be modelled accurately using the above approaches, artificial neural networks (ANNs) were investigated since they have previously been shown to be applicable to complex CE systems [18–20] having a range of input and output parameters.

For the current system the three variables, %PVS, [β-CD] and pH were used as the input layer while the 13 mobilities (one for each analyte) were used as the output layer. The structure of the ANN was optimised by varying the number of hidden layers and nodes and the best architecture was determined to be three input parameters, two hidden layers comprising 20 nodes each and the 13 output parameters.

The ANN was trained with the full data set of 21 points and was then used to predict optimum separations using both the normalised resolution product and minimum resolution criteria. The same iterative optimisation procedure used earlier was again employed. Predicted optimal conditions were 0.3% PVS, 0 m*M* β-CD at pH 3.75 for the normalised resolution product. Agreement between predicted and observed migration times was less than 1.4% for the conditions calculated using the normalised resolution product criterion and less than 4.2% for the minimum resolution criterion. In the case of optimisation using the minimum resolution criterion it was necessary to constrain the calculations to accept only analyte mobilities greater than $2 \cdot 10^{-9}$ m^2 V^{-1} s^{-1} in order to avoid overlap of analyte peaks with the large negative baseline disturbance caused by the EOF peak. This ensured that all peaks in the resultant electropherogram were well separated from the EOF. The optimal conditions calculated using this modified criterion were 0.9% PVS, 5 m*M* β-CD at pH 3.50 and observed migration times under these conditions agreed with predicted values to within 1.5%. Separations obtained using the optimal conditions for both optimisation criteria are shown in Fig. 7. Both approaches yielded good separations with most of the peaks being resolved fully. It is also interesting to note that both optima utilise low pH

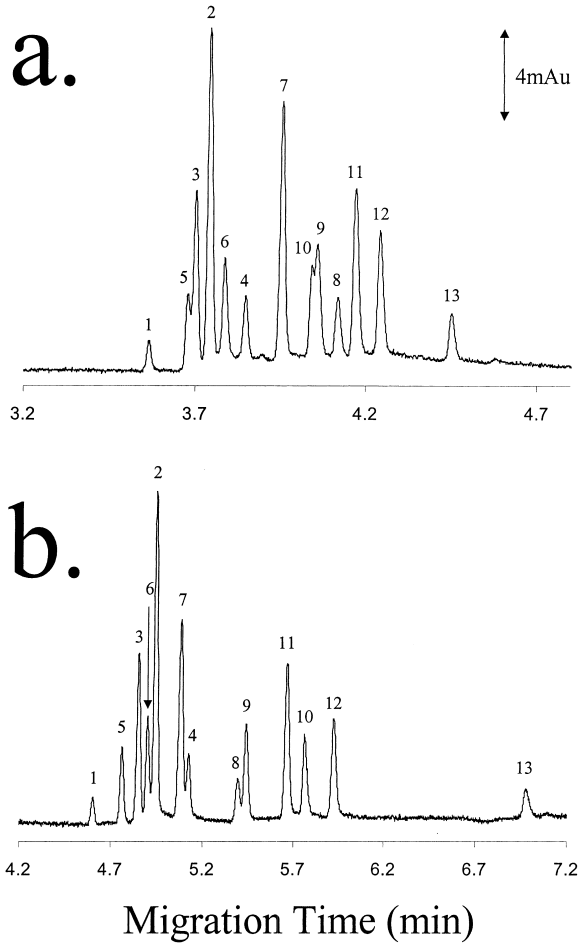

Fig. 7. Optimum separations calculated with the ANN and using (a) the normalised resolution product criterion and (b) the minimum resolution criterion with the additional constrain that all mobilities must be greater than $2 \cdot 10^{-9}$ m^2 V^{-1} s^{-1}. Conditions: (a) 0.3% PVS, 0 m*M* β-CD at pH 3.75; (b) 0.9% PVS, 5 m*M* β-CD at pH 3.50. Peaks are: 1 = pyridine, 2 = *m*-aminopyridine, 3 = *p*-aminopyridine, 4 = *o*-aminopyridine, 5 = picoline, 6 = ethylpyridine, 7 = quinoline, 8 = aniline, 9 = benzylamine, 10 = *tert*.-butylpyridine, 11 = methylbenzylamine, 12 = ethylaniline and 13 = pentylaniline. General conditions: 20 m*M* citrate, detection at 211 nm.

conditions (3.75 and 3.50) which are very close to the fixed pH used in the simplified model (3.50). This suggests that the ability to vary pH for this particular set of analytes pH did not significantly influence the ability to separate the analytes. That is, introduction of a three-dimensional experimental space in this example offered little improvement over the two-dimensional experimental space.

3.9. Selectivity manipulation

The major advantage in having several independent interactions operating within a system is the increased selectivity control that can be achieved. This offers advantages where co-migration of analytes is a problem or where peaks are masked by other components present in the sample at much larger concentrations. As an example, the peaks for aniline and benzylamine can be considered. As mentioned above and shown in Table 2, these two analytes showed very similar mobilities and interactions with both the pseudo-SPs and their separation can therefore be expected to be difficult. By using the ANN model of the three-dimensional system, it is possible to predict the conditions needed to obtain the separation for a desired migration order of these analytes. This is shown in Fig. 8 where aniline migrated before benzylamine under the conditions shown in Fig. 8a, and in the reverse migration order under the conditions shown in Fig. 8b. The optimal separation with aniline migrating before benzylamine was achieved with protonated analytes (pH 3.50) and selecting appropriate values of %PVS and [β-CD]. On the other hand, the reverse migration order could be accomplished using only pH control in the absence of both pseudo-SPs. These very diverse conditions were predicted accurately and rapidly by the ANN. This process could be extended readily to a much wider range of analytes.

4. Conclusions

The multi-mode EKC system consisting of polyvinylsulfonate and β-CD as pseudo-SPs combines ion-exchange and hydrophobic interactions as two complementary chromatographic separation mechanisms with an electrophoretic separation. The extent of each interaction can be varied independently by changing the concentration of each pseudo-SP. A mathematical model has been derived which accurately describes the analyte mobilities with differing BGE conditions. This model can also be used to successfully optimise the system. The addition of pH

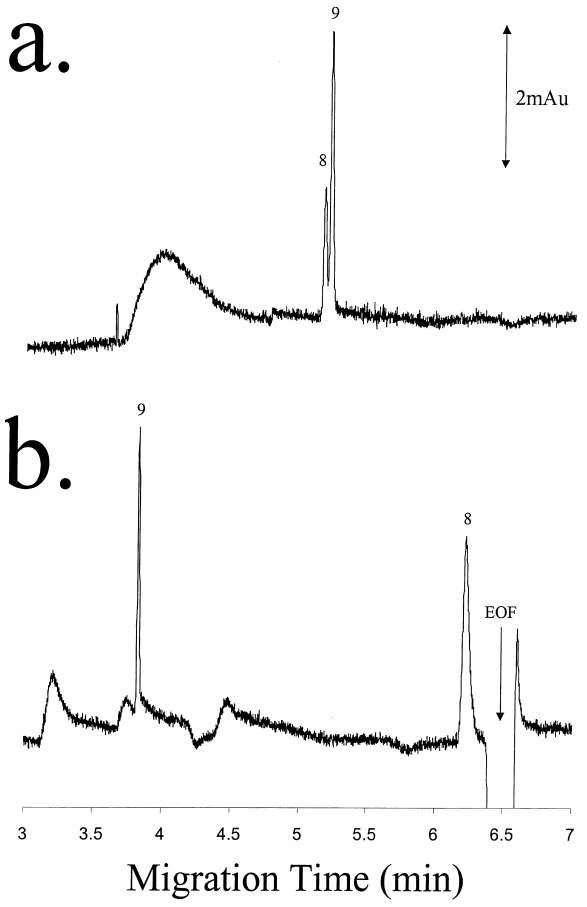

Fig. 8. Selectivity control offered over aniline and benzylamine. (a) Aniline migrating before benzylamine and (b) benzylamine migrating before aniline. Conditions: (a) 0.6% PVS, 7 m*M* β-CD at pH 3.50 and (b) 0% PVS, 0 m*M* β-CD at pH 5.75. Peaks are 8 = aniline and 9 = benzylamine. General conditions: 20 m*M* citrate, detection at 211 nm.

as a further experimental parameter limits the application of a physical migration model. However, an artificial neural network was shown to be applicable to this three-dimensional system and was utilised for the selection of conditions providing the best overall separation or the achievement of a desired migration order. Although a reasonably large number of experimental data points was needed to successfully train the artificial neural network, the resultant performance was better than that obtained using the same number of experiments to solve the full mathematical migration model.

The described system is potentially applicable to any analytes that exhibit interactions with PVS and/or β-CD. The system can also be readily modified to suit a particular set of analytes by utilising different pseudo-SPs. One particular area of application could be in the analysis of pharmaceutically important compounds, since many of these are aromatic bases. The presence of the cyclodextrin could also facilitate the enantiomeric separation while the PVS could aid the electrophoretic separation of different compounds showing very similar electrophoretic mobilities.

References

[1] R. Kuhn, S. Hoffstetter-Kuhn, Capillary Electrophoresis: Principles and Practice, Springer, Berlin, 1993.
[2] T. de Boer, R.A. de Zeeuw, G.J. de Jong, K. Ensing, Electrophoresis 20 (1999) 2989.
[3] A. Bunke, T. Jira, J. Chromatogr. A 798 (1998) 275.
[4] S. Izumoto, H. Nishi, Electrophoresis 20 (1999) 189.
[5] P. Zakaria, M. Macka, P.R. Haddad, Anal. Chem. 74 (2002) 1241.
[6] J. Li, J.S. Fritz, J. Chromatogr. A 840 (1999) 269.
[7] E. Minnoor, Y. Liu, D.J. Pietrzyk, J. Chromatogr. A 884 (2000) 297.
[8] P. Bednar, Z. Stransky, P. Bartak, P. Adamovsky, J. Chromatogr. A 838 (1999) 89.
[9] S. Takeda, S. Wakida, M. Yamane, Z. Siroma, K. Higashi, S. Terabe, J. Chromatogr. A 817 (1998) 59.
[10] C.M. Knapp, J.J. Breen, J. Chromatogr. A 799 (1998) 289.
[11] W.C. Brumley, W.J. Jones, J. Chromatogr. A 680 (1994) 163.
[12] S. Takeda, S. Wakida, M. Yamane, A. Kawahara, K. Higashi, J. Chromatogr. A 653 (1993) 109.
[13] H. Katayama, Y. Ishihama, N. Asakawa, Anal. Chem. 70 (1998) 2254.
[14] P. Zakaria, M. Macka, P.R. Haddad, Electrophoresis 23 (2002) 1844.
[15] M.C. Breadmore, P.R. Haddad, J.S. Fritz, Electrophoresis 21 (2000) 3181.
[16] P. Zakaria, M. Macka, P.R. Haddad, J. Chromatogr. A 985 (2003) 493.
[17] J. Snopek, I. Jelinek, E. Smolkova-Keulemansova, J. Chromatogr. 452 (1988) 571.
[18] J. Havel, E.M. Pena, A. Rojas-Hernandez, J.-P. Doucet, A. Panaye, J. Chromatogr. A 793 (1998) 317.
[19] L. Pokorna, A. Revilla, J. Havel, J. Patocka, Electrophoresis 20 (1999) 1993.
[20] M. Pacheco, J. Havel, Electrophoresis 23 (2002) 268.